JACS
JOURNAL OF THE AMERICAN CHEMICAL SOCIETY

Article

A Direct Comparison of One- and Two-Component Dendritic Self-Assembled Materials: Elucidating Molecular Recognition Pathways

Buqing Huang, Andrew R. Hirst, David K. Smith, Valeria Castelletto, and Ian W. Hamley

J. Am. Chem. Soc., **2005**, 127 (19), 7130-7139• DOI: 10.1021/ja050412d • Publication Date (Web): 23 April 2005

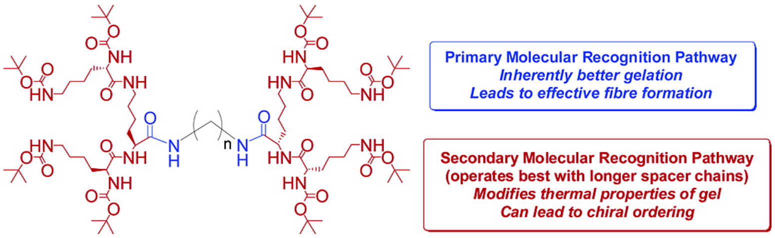

ACS Publications
High quality. High impact.

Journal of the American Chemical Society is published by the American Chemical Society. 1155 Sixteenth Street N.W., Washington, DC 20036

J|A|C|S
ARTICLES

A Direct Comparison of One- and Two-Component Dendritic Self-Assembled Materials: Elucidating Molecular Recognition Pathways

Buqing Huang,[†] Andrew R. Hirst,[†] David K. Smith,*,[†] Valeria Castelletto,[‡] and Ian W. Hamley[‡]

*Contribution from the Department of Chemistry, University of York,
Heslington, York YO10 5DD, UK, and Department of Chemistry, University of Leeds,
Leeds, West Yorkshire LS2 9JT, UK*

Received January 21, 2005; E-mail: dks3@york.ac.uk

Abstract: This paper compares and contrasts, for the first time, one- and two-component gelation systems that are direct structural analogues and draws conclusions about the molecular recognition pathways that underpin fibrillar self-assembly. The new one-component systems comprise L-lysine-based dendritic headgroups covalently connected to an aliphatic diamine spacer chain via an amide bond. One-component gelators with different generations of headgroup (from first to third generation) and different length spacer chains are reported. The self-assembly of these dendrimers in toluene was elucidated using thermal measurements, circular dichroism (CD) and NMR spectroscopies, scanning electron microscopy (SEM), and small-angle X-ray scattering (SAXS). The observations are compared with previous results for the analogous two-component gelation system in which the dendritic headgroups are bound to the aliphatic spacer chain noncovalently via acid−amine interactions. The one-component system is inherently a more effective gelator, partly as a consequence of the additional covalent amide groups that provide a new hydrogen bonding molecular recognition pathway, whereas the two-component analogue relies solely on intermolecular hydrogen bond interactions between the chiral dendritic headgroups. Furthermore, because these amide groups are important in the assembly process for the one-component system, the chiral information preset in the dendritic headgroups is not always transcribed into the nanoscale assembly, whereas for the two-component system, fiber formation is always accompanied by chiral ordering because the molecular recognition pathway is completely dependent on hydrogen bond interactions between well-organized chiral dendritic headgroups.

Introduction

Rationally designed molecules that self-assemble to form nanoscale architectures are of crucial importance in the emergent field of nanochemistry.[1] Building on the fundamental principles of supramolecular chemistry,[2] appropriately designed systems may interact through the formation of complementary noncovalent interactions such as hydrogen bonds, electrostatic interactions, solvophobic forces, $\pi-\pi$ stacking interactions, van der Waals forces, etc. Gel-phase materials[3] offer an exciting arena for exploring the ways in which molecular recognition pathways can transcribe "information" from the molecular level up to the nanoscale and, ultimately, its expression on the macroscopic scale in terms of materials properties. The vast majority of gel-phase materials are one-component systems in which the gelator molecules self-recognize, forming supramolecular "polymer-like" structures.[4] Dendritic molecules have been of particular interest as gelators[5] because multiple noncovalent interactions between dendrons or dendrimers are possible as a consequence of the multiple repeat groups inherent within the branched superstructure, and the steric bulk of the

---

[†] University of York.

[‡] University of Leeds.

(1) (a) Whitesides, G. M.; Grzybowski, B. *Science* **2002**, *295*, 2418−2421. (b) Hamley, I. W. *Angew. Chem., Int. Ed.* **2003**, *42*, 1692−1712.

(2) (a) Beer, P. D.; Gale, P. A.; Smith, D. K. *Supramolecular Chemistry*; Oxford University Press: Oxford, U.K., 1999. (b) Steed, J. W.; Atwood, J. L. *Supramolecular Chemistry*; John Wiley and Sons: Chichester, U.K., 2000.

(3) (a) Terech, P.; Weiss, R. G. *Chem. Rev.* **1997**, *97*, 3133−3159. (b) Gronwald, O.; Snip, E.; Shinkai, S. *Curr. Opin. Colloid Interface Sci.* **2002**, *7*, 148−156. (c) van Esch, J. H.; Feringa, B. L. *Angew. Chem., Int. Ed.* **2000**, *39*, 2263−2266. (d) Oda, R.; Huc, I.; Candau, S. J. *Angew. Chem., Int. Ed.* **1998**, *37*, 2689−2691. (e) Abdallah, D. J.; Weiss, R. G. *Adv. Mater.* **2000**, *12*, 1237−1247. (f) Shimizu, T. *Polymer J.* **2003**, *35*, 1−22.

(4) Brunsveld, L.; Folmer, J. B.; Meijer, E. W.; Sijbesma, R. P. *Chem. Rev.* **2001**, *101*, 4071−4097.

(5) For a review, see: (a) Hirst, A. R.; Smith D. K. *Top. Curr. Chem.* **2005**, in press. For examples, see: (b) Newkome, G. R.; Baker, G. R.; Saunders: M. J.; Russo, P. S.; Gupta, V. K.; Yao, Z. Q.; Miller, J. E.; Bouillion, K. *J. Chem. Soc., Chem. Commun.* **1986**, 752−753. (c) Newkome, G. R.; Baker, G. R.; Arai, S.; Saunders: M. J.; Russo, P. S.; Theriot, K. J.; Moorefield, C. N.; Rogers, L. E.; Miller, J. E.; Lieux, T. R.; Murray, M. E.; Phillips, B.; Pascal, L. *J. Am. Chem. Soc.* **1990**, *112*, 8458−8465. (d) Newkome, G. R.; Moorefield, C. N.; Baker, G. R.; Behera, R. K.; Escamilla, G. H.; Saunders: M. J. *Angew. Chem., Int. Ed. Engl.* **1992**, *31*, 917−919. (e) Jang, W.-D.; Jiang, D.-L.; Aida, T. *J. Am. Chem. Soc.* **2000**, *122*, 3232−3233. (f) Jang, W.-D.; Aida, T. *Macromolecules* **2003**, *36*, 8461−8469. (g) Kim, C.; Kim, K. T.; Chang, Y.; Song, H. H.; Cho, T.-Y.; Jeon, H.-J. *J. Am. Chem. Soc.* **2001**, *123*, 5586−5587. (h) Kim, C.; Lee, S. J.; Lee, I. H.; Kim, K. T.; Song, H. H.; Jeon, H.-J. *Chem. Mater.* **2003**, *15*, 3638−3642. (i) Marmillon, C.; Gauffre, F.; Gulik-Krzywicki, T.; Loup, C.; Caminade, A.-M.; Majoral, J.-P.; Vors, J.-P.; Rump, E. *Angew. Chem., Int. Ed.* **2001**, *40*, 2626−2629. (j) Zhang, W.; Gonzalez, S. O.; Simanek, E. E. *Macromolecules* **2002**, *35*, 9015−9021. (k) Zubarev, E. R.; Pralle, M. U.; Sone, E. D.; Stupp, S. I. *J. Am. Chem. Soc.* **2001**, *123*, 4105−4106.

10.1021/ja050412d CCC: $30.25

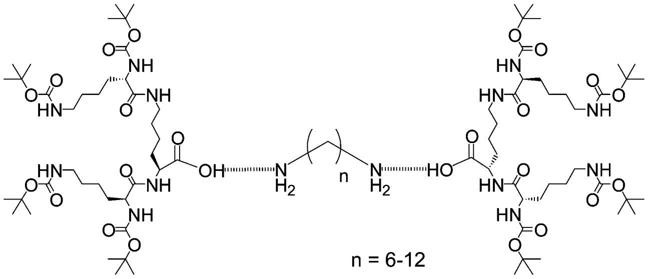

Figure 1. Two-component dendritic gelation system (**G2···C*n*···G2**) previously reported by us.[7−13]

dendritic units can help enforce directionality on the assembly process. In recent years, systems in which two components are required for gelation have come under increasing scrutiny.[6] In such systems, it can be considered that a prerequisite for nanoscale assembly is the formation of a "host−guest" complex between the two components. It is this complex that hierarchically self-assembles to form extended nanoscale aggregates.

In 2001, we first reported a novel two-component dendritic gelation system (Figure 1),[7] in which dendritic headgroups based on L-lysine with a carboxylic acid at the focal point interact with and solubilize an aliphatic diamine. The complex that forms as a consequence of acid−base interactions hierarchically self-assembles in an anisotropic manner to form fibers, generating a sample-spanning network that underpins macroscopic gelation. We have recently reported detailed studies of this system and highlighted the roles of the spacer chain,[8] dendritic generation,[9] solvent,[10] stereochemistry,[11] ratio of the two components,[12] and surface groups[13] in controlling self-assembly. The complexes self-assemble into helical fibers, with adjacent complexes (and hence the fibers) held together by intermolecular dendron−dendron hydrogen bond interactions. The host−guest complex can also be formed using interactions between dendritic crown ethers and a protonated aliphatic diamine; gelation still ensues.[14]

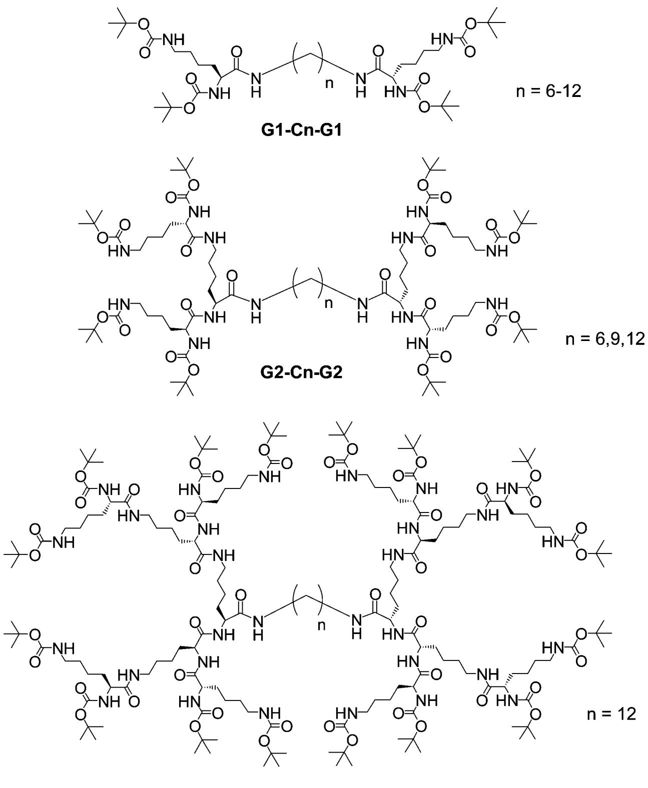

Figure 2. Novel one-component gelators (**G*m*-C*n*-G*m***) reported in this paper.

We realized that our two-component system provided a unique opportunity for comparison against structurally analogous one-component gelators in which the dendritic headgroups are permanently connected to the aliphatic diamine via covalent peptide bond linkages (Figure 2).[15] As such, this paper provides an insight into differences between one- and two-component gelators, their modes of self-assembly, and the molecular recognition events that underpin gelation. Understanding the molecular recognition pathways that underpin self-assembly is of key importance both in materials chemistry and in biological systems.

We report the one-component (covalent) analogues of the two-component gelation system, with varied structural (molecular scale) information in two key regions: (a) *dendritic generation* and (b) *spacer chain*. Importantly, we can understand and differentiate the different hydrogen bonding molecular recognition pathways that give rise to both gelation and nanoscale chiral organization.

Results and Discussion

Synthesis of Novel One-Component Gelators. The one-component dendritic gelators (Figure 2) were synthesized

---

(6) Two-component gels based on hydrogen bonding: (a) Hanabusa, K.; Miki, T.; Taguchi, Y.; Koyama, T.; Shirai, H. *J. Chem. Soc., Chem. Commun.* **1993**, 1382−1384. (b) Jeong, S. W.; Shinkai, S. *Nanotechnology*, **1997**, *8*, 179−185. (c) Inoue, K.; Ono, Y.; Kanekiyo, Y.; Ishi-i, T.; Yoshihara, K.; Shinkai, S. *J. Org. Chem.* **1999**, *64*, 2933−2937. (d) Xu, X.; Ayyagari, M.; Tata, M.; John, V. T.; McPherson, G. L. *J. Phys. Chem.* **1993**, *97*, 11350−11353. (e) Tata, M.; John, V. T.; Waguespack, Y. Y.; McPherson, G. L. *J. Am. Chem. Soc.* **1994**, *116*, 9464−9470. (f) Waguespack, Y. Y.; Banerjee, S.; Ramannair, P.; Irvin, G. C.; John, V. T.; McPherson, G. L. *Langmuir* **2000**, *16*, 3036−3041. (g) Simmons, B. A.; Taylor, C. E.; Landis, F. A.; John, V. T.; McPherson, G. L.; Schwartz, D. K.; Moore, R. *J. Am. Chem. Soc.* **2001**, *123*, 2414−2421. (h) Willemen, H. M.; Vermonden, T.; Marcelis, A. T. M.; Sudhölter, E. J. R. *Langmuir* **2002**, *18*, 7102−7106. (i) de Loos, M.; van Esch, J.; Kellogg, R. M.; Feringa, B. L. *Angew. Chem., Int. Ed.* **2001**, *40*, 613−616. (j) Nakano, K.; Hishikawa, Y.; Sada, K.; Miyata, M.; Hanabusa, K. *Chem. Lett.* **2000**, 1170−1171. Two-component gels based on donor−acceptor interactions: (k) Maitra, U.; Kumar, P. V.; Chandra, N.; D'Sousa, L. J.; Prasanna, M. D.; Raju, A. R. *Chem. Commun.* **1999**, 595−596. (l) Friggeri, A.; Gronwald, O.; van Bommel, K. J. C.; Shinkai, S.; Reinhoudt, D. N. *J. Am. Chem. Soc.* **2002**, *124*, 10754−10758. (m) Babu, P.; Sangeetha, N. M.; Vijaykumar, P.; Maitra, U.; Rissanen, K.; Raju, A. R. *Chem. Eur. J.* **2003**, *9*, 1922−1932. Two-component gels based on a reversible chemical reaction give rise to latent gels: (n) George, M.; Weiss, R. G. *Langmuir* **2003**, *19*, 1017−1025. (b) George, M.; Weiss, R. G. *Langmuir* **2002**, *18*, 7124−7135. Irreversible chemical reactions can also be used to generate gel-phase materials in situ: (o) Suzuki, M.; Nakajima, Y.; Yumoto, M.; Kimua, M.; Shirai, H.; Hanabusa, K. *Langmuir* **2003**, *19*, 8622−8624. (p) Suzuki, M.; Nakajima, Y.; Yumoto, M.; Kimura, M.; Shirai, H.; Hanabusa K. *Org. Biomol. Chem.* **2004**, *2*, 1155−1159. Two-component gels in which interaction of a ligand component with a metal ion modifies the properties of the gel-phase materials: (q) Ihara, H.; Sakurai, T.; Yamada, T.; Hashimoto, T.; Takafuji, M.; Sagaura, T.; Hachisako, H. *Langmuir* **2002**, *18*, 7120−7123. (r) Dukh, M.; Saman, D.; Kroulik, J.; Cerny, I.; Pouzar, V.; Kral, V.; Drasar, P. *Tetrahedron* **2003**, *59*, 4069−4076.

(7) (a) Partridge, K. S.; Smith, D. K.; Dykes, G. M.; McGrail, P. T. *Chem. Commun.* **2001**, 319−320.

(8) Hirst, A. R.; Smith, D. K.; Feiters, M. C.; Geurts, H. P. M. *Langmuir* **2004**, *20*, 7070−7077.

(9) Hirst, A. R.; Smith, D. K. *Org. Biomol. Chem.* **2004**, *2*, 2965−2971.

(10) Hirst, A. R.; Smith, D. K. *Langmuir* **2004**, *20*, 10851−10857.

(11) Hirst, A. R.; Smith, D. K. Feiters, M. C.; Geurts, H. P. M. *Chem. Eur. J.* **2004**, *10*, 5901−5910.

(12) Hirst, A. R.; Smith, D. K.; Feiters, M. C.; Geurts, H. P. M.; Wright, A. C. *J. Am. Chem. Soc.* **2003**, *125*, 9010−9011.

(13) Hardy, J. G.; Hirst, A. R.; Smith, D. K.; Ashworth, I.; Brennan, C. *Chem. Commun.* **2005**, 385−387.

(14) Dykes, G. M.; Smith, D. K. *Tetrahedron* **2003**, *59*, 3999−4009.

(15) Love, C. S.; Hirst, A. R.; Chechik, V.; Smith D. K.; Ashworth I.; Brennan C. *Langmuir* **2004**, *20*, 6580−6585.

Scheme 1. Synthesis of one-component dendritic gelators (**G*m*-C*n*-G*m***) using a divergent approach[a]

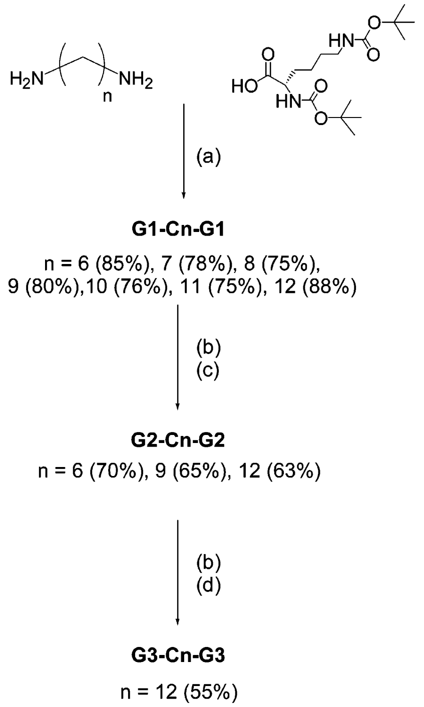

[a] Reagents and conditions: (a) DCC, HOBt, NEt_3 EtOAc, 24 h; (b) CF_3COOH, CH_2Cl_2, 30 min; (c) DCC, HOBt, NEt_3, EtOAc, 3 d; (d) EDC, HOBt, DMAP, CH_2Cl_2, 5 d.

according to Scheme 1. A divergent approach was used in order to maintain the stereochemical integrity of the L-lysine[16] amino acid building blocks.[17] This was important as we have recently shown that the stereochemistry of dendritic gelators has a significant impact on their self-assembly.[11] The first generation dendrimers **G1-C*n*-G1** ($n = 6-12$) were generated by coupling Boc-protected L-lysine[18] to the appropriate diaminoalkanes using 1,3-dicyclohexylcarbodiimide (DCC) and 1-hydroxybenzotriazole (HOBt) in the presence of triethylamine (NEt_3) as base and ethyl acetate (EtOAc) as solvent. The products, which precipitated from the reaction mixture along with the dicyclohexylurea (DCU) side product, could be extracted from the solid mixture and subsequently purified by silica column chromatography. All first generation systems were formed in excellent yields (75−88%) using this approach.

Deprotection of the first generation systems **G1-C6-G1**, **G1-C9-G1**, and **G1-C12-G1** was achieved using trifluoroacetic acid, followed by in situ DCC/HOBt-mediated coupling to a slight excess of Boc-protected L-lysine in order to provide second generation dendrimers **G2-C6-G2**, **G2-C9-G2**, and **G2-C12-G2**. These products were purified by gel permeation chromatography (GPC, Biobeads, SX-1) or silica column chromatography as appropriate and were obtained in good yields (62−70%).

Table 1. Ability of Dendritic Gelators to Form Gel-Phase Materials in Different Solvents at a Mass Loading of 1% w/v (i.e., 10 mg/mL)[a]

	toluene	hexane	cyclohexane	$CHCl_3$	CH_2Cl_2	methanol
G1-C12-G1	G	CG	CG	S	S	S
G2-C12-G2	G	CG	CG	G	PG	S
G3-C12-G3	G	CG	CG	G	G	S

[a] G = gel, PG = partial gel (partial immobilization of the solvent was observed but complete macroscopic immobilization did not occur, i.e., there was some fluidity on tube inversion), CG = cloudy gel, S = solution.

Finally, **G2-C12-G2** was deprotected using trifluoroacetic acid and subsequently coupled to an excess of Boc-protected L-lysine. This time, however, 1-(3-dimethylaminopropyl)-3-ethylcarbodiimide hydrochloride (EDC) was employed as coupling agent in the presence of HOBt and using 4-(dimethylamino)pyridine (DMAP) as base. Purification by preparative GPC (Sephadex LH-20, MeOH) provided third generation dendrimer **G3-C12-G3** in a useful 55% yield.

All of the novel dendrimers were characterized by appropriate analytical methods to provide evidence of purity and identity (see Experimental Section and Supporting Information for details). In the following sections, we describe the effects of (a) *dendritic generation* and (b) *spacer chain* on the self-assembly of gel-phase materials. Comparison with the data for the analogous two-component gelation systems allows us to unambiguously assign the molecular recognition pathways that operate and the impact they have on chiral nanoscale organization.

Characterization of the Novel Gel-Phase Materials. (a) Effect of Dendritic Branching. For this study, we compared the gel-phase materials formed by **G1-C12-G1**, **G2-C12-G2**, and **G3-C12-G3**. Initially, the ability of the dendrimers to structure a small selection of solvents was investigated (Table 1). Aromatic apolar solvents (e.g., toluene) were gelated by all three generations of dendrimer, and in each case an optically transparent gel was formed, which indicates good solubility of the dendrimer and resultant nanoscale assemblies. Aliphatic apolar solvents (e.g., cyclohexane and hexane), however, formed cloudy gels, indicating that solubility was poor or that the aggregates that formed in these solvents were capable of scattering light. These solvents were not investigated further here. Hydrogen bonding solvents (e.g., methanol) solubilized the dendrimers and showed no evidence of sample-spanning structuring, consistent with intermolecular hydrogen bonding between dendritic headgroups being a prerequisite for macroscopic gelation. Most interesting, however, were chlorinated solvents (e.g., CH_2Cl_2 and $CHCl_3$), which are moderately polar and have some hydrogen bond donor ability. First generation **G1-C12-G1** was unable to gelate these solvents, but on increasing the dendritic branching to **G2** and **G3**, gelation did become possible. This indicates that in these intermediate solvents, the higher generation dendrimers are significantly better gelators. Potential reasons for this apparent *positive* dendritic effect up to the third generation will be discussed in more detail below.

We assessed the three gelators in more detail, by studying the transition from an immobile to a mobile self-assembled state in toluene using tube inversion experiments. This method served

---

(16) For the original report of dendrimers based on L-lysine, see: (a) Denkewalter, R. G.; Kolc, J.; Lukasavage, W. J.; Allied Corp; U.S. Patent 4,289,872, 1981; *Chem. Abstr.* **1985**, *102*, 79324q. A number of other gel-phase materials based on L-lysine have been reported; see for example: (b) Hanabusa, K.; Nakayama, H.; Kimura, M.; Shirai H. *Chem. Lett.* **2000**, 1070−1071. (c) Suzuki, M.; Yumoto, M.; Kimura H.; Shirai, H.; Hanabusa, K. *Helv. Chim. Acta* **2004**, *87*, 1−10 and references therein.

(17) (a) Dykes, G. M.; Brierley, L. J.; Smith, D. K.; McGrail, P. T., Seeley, G. J. *Chem. Eur. J.* **2001**, *7*, 4730−4739. (b) Driffield, M.; Goodall, D. M.; Smith, D. K. *Org. Biomol. Chem.* **2003**, *1*, 2612−2620.

(18) Boc-protected L-lysine was synthesised according to: Keller, O.; Keller, W. E.; van Look, G.; Wersin, G. *Org. Synth.* **1985**, *63*, 160−170.

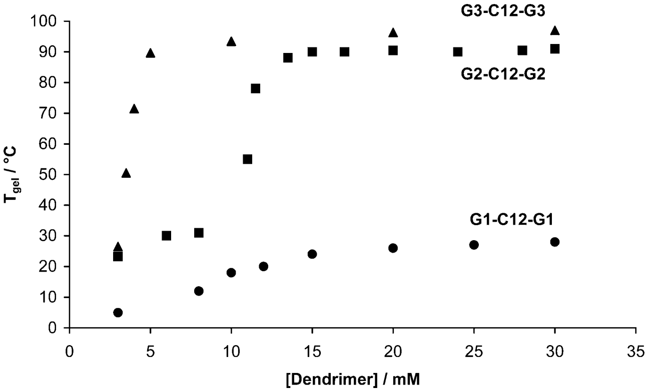

Figure 3. Effect of [dendrimer] on the gel−sol transition temperature (T_{gel}) for **G*m*-C12-G*m*** as measured by tube-inversion methodology. Solvent = toluene.

to define a mobile-gel transition temperature (i.e., a gel “boundary”) and is described in detail in the Experimental Section (the method is highly reproducible and the estimated error is ±1 °C).[19] This gel boundary is analogous to the thermally reversible gel-sol transition temperature (T_{gel}). T_{gel} values were measured at different concentrations of gelator (Figure 3). As previously reported for the two-component systems,[7−13] when the molar concentration of the gelators was increased, the T_{gel} values also increased, until a concentrated regime (the “plateau region”) was reached, denoted by a concentration-independent T_{gel}.

It is noteworthy that all of the dendritic materials formed gel-phase materials, even the first generation system **G1-C12-G1**. The first generation compound has a T_{gel} value of 34 °C in the plateau region (at a concentration of 60 mM), a value that increases to 92 °C for **G2-C12-G2** and 97 °C for **G3-C12-G3**. Therefore, for **G*m*-C12-G*m*** there is a *positive* dendritic effect up to the third generation. In other words, increasing the size of the dendritic headgroups increases the thermal stability of the gel in the plateau region. In addition, the concentration of dendrimer required to induce macroscopic gelation decreased with increasing generation. This effect is greater than might simply be expected on the basis of the fact that the larger molecular mass of the higher generation dendrimers will increase the apparent weight percent per volume. This again indicates that the higher generation dendrimers have a greater propensity to structure toluene.

The most likely explanation for these *positive* dendritic effects up to the third generation is that additional hydrogen bonds are possible for the higher generation systems. This would also explain why the higher generation systems were better able to gelate solvents such as CH_2Cl_2 and $CHCl_3$ (Table 1). In addition, the amide hydrogen bonding groups responsible for gelation will be more shielded from the solvent as the dendritic generation increases. It might be anticipated that if dendritic functionalization was increased even further, this dendritic effect may not continue, as steric factors should become increasingly dominant with larger dendritic structures, hindering anisotropic self-assembly.

It is also interesting to note that the plot of T_{gel} for the second generation system has an unusual sigmoidal shape. This may indicate the formation of a moderately stable gel phase in the low concentration regime. Similar behavior was previously observed for the two-component system.[9] This paper, however, generally focuses on the behavior of these materials in the concentrated regime; a more detailed survey of the interesting materials behavior at lower concentrations is currently in progress.

Differential scanning calorimetry (DSC) was used to confirm the approximate T_{gel} values for **Gn-C12-Gn** (Supporting Information, Figure S1). The first and second generation dendrimers gave rise to fairly sharp reproducible endotherms at 50 and 100 °C, respectively. For the third generation system, however, a very broad endotherm was observed with a maximum at ca. 98 °C. This broad trace may indicate that for **G3-C12-G3**, the transition from an immobile self-assembled state to one that is mobile is less cooperative. It is possible that although this gel has relatively good thermal stability, it is actually less ordered on the molecular level. In other words, although dendrimer **G3-C12-G3** can form multiple hydrogen bond interactions between dendritic headgroups (providing the gel with thermal stability), these may be relatively disorganized in spatial terms.

NMR techniques can provide a large amount of information relating to the self-assembly of the gel state.[20] Variable-temperature ^{1}H NMR spectroscopy was initially performed, and compound **G1-C12-G1** exhibited NMR signals across the entire temperature range. Increasing the temperature led to an upfield shift in the NMR signals, particularly those corresponding to the N−H protons. This indicates that these protons are involved in dendrimer-dendrimer hydrogen bonding interactions that are broken on increasing temperature. **G2-C12-G2**, a more effective gelator than **G1-C12-G1**, exhibited no measurable ^{1}H NMR signals at ambient temperature because of the lack of molecular mobility in the gel. Only at elevated temperatures (ca. 60 °C) were NMR signals observed. These signals sharpened and shifted upfield on increasing the temperature further, again consistent with hydrogen bonding. Practical difficulties made it impossible to prepare an NMR sample of **G3-C12-G3** at an appropriate concentration.

To explore the hydrogen bond interactions further, we monitored the NMR spectrum of **G1-C12-G1** at 20 °C as a function of concentration. On increasing the concentration of the gelator, the N−H peaks shifted downfield, consistent with the formation of intermolecular hydrogen bond interactions (Figure 4). This proves that it is dendrimer-dendrimer hydrogen bond interactions that underpin gel formation as the sample concentration increases. Most interestingly, the N−H signals of the “new” covalent amide protons that link the spacer chain to the dendritic headgroups were much more strongly perturbed ($\Delta\delta$ = 0.65 ppm) than those of the carbamates ($\Delta\delta$ = 0.26 ppm). Intermolecular hydrogen bonding via the amide groups is therefore probably the primary molecular recognition pathway

---

(19) (a) Chaibundit, C.; Shao-Min, M.; Heatley, F.; Booth, C. *Langmuir* **2000**, *16*, 9645−9652. (b) Kelarakis, A.; Yang, Z.; Pousia, E.; Nixon, S. K.; Price, C.; Booth, C.; Hamley, I. W.; Castelletto, V.; Fundin, J. *Langmuir* **2001**, *17*, 8085−8091.

(20) (a) Murata, K.; Aoki, M., Suzuki, T.; Harada, T.; Kawabata, H.; Komori, T.; Ohseto, F.; Ueda, K.; Shinkai, S. *J. Am. Chem. Soc.* **1994**, *116*, 6664−6676. (b) Schoonbeek, F. S.; van Esch, J. H.; Hulst, R.; Kellogg, R. M.; Feringa, B. L. *Chem. Eur. J.* **2000**, *6*, 2633−2643. (c) Amanokura, N.; Yoza, K.; Shinmori, H,; Shinkai, S.; Reinhoudt, D. N. *J. Chem. Soc., Perkin. Trans. 2* **1998**, 2585−2591. (d) Yoza, K.; Amanokura, N.; Ono, Y.; Akao, T.; Shinmori, H. Takeuchi, M.; Shinkai, S.; Reinhoudt, D. N. *Chem. Eur. J.* **1999**, *5*, 2722−2729. (e) Duncan, D. C.; Whitten, D. G. *Langmuir* **2000**, *16*, 6445−6452. (f) Tata, M.; John, V. T.; Waguespack, Y. Y.; McPherson, G. L. *J. Phys. Chem.* **1994**, *98*, 3809−3817. (g) Camerel, F.; Faul, C. F. J. *Chem. Commun.* **2003**, 1958−1959.

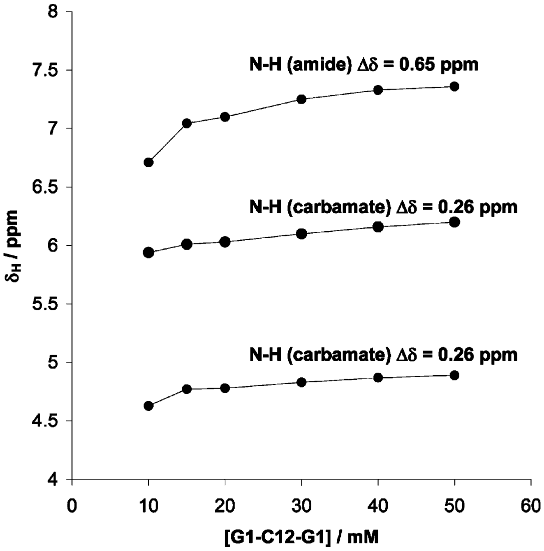

Figure 4. Concentration dependence of the N−H resonances in the NMR spectra of **G1-C12-G1**. All spectra measured at 20 °C. Solvent = toluene-d_8. $\Delta\delta$ values refer to the change in NMR shift on increasing the concentration from 10 to 50 mM.

directing the self-assembly process that underpins macroscopic gelation, with the carbamates in the dendritic headgroups playing a supporting or secondary role.

Circular dichroism (CD) spectroscopy[21] is an ideal method for probing the supramolecular organization of chiral molecules.[22] CD spectra were therefore measured (Supporting Information, Figure S2, [dendrimer] = 3 mM, solvent = cyclohexane). For **G1-C12-G1** and **G2-C12-G2** the peak maxima were at ca. 220 nm, ascribable to the amide carbonyl group of the dendritic peptides being organized into a supramolecular extended helical conformation. For **G3-C12-G3**, however, the $\lambda_{\max}$ value was shifted to 210 nm, which may indicate a different organization of the multiple amide groups. In each case, the CD band had the same negative sign, indicating the bias of the organized supramolecular chirality has the same directionality in each case. The intensity of the CD band was ca. −130, −120, and −105 for **G1**, **G2**, and **G3** systems, respectively. It may have been expected that the increasing number of amide groups as dendritic generation increases would lead to an increasing CD signal. This CD data, in which the **G3** system shows less chiral order than may have been expected and a different $\lambda_{\max}$ value, is in agreement with the DSC data, which indicated that although **G3-C12-G3** has the most hydrogen bonding groups, these hydrogen bond interactions are relatively spatially disorganized.

Molecular self-assembly at the nanoscale level was probed using scanning electron microscopy (SEM), a useful comparative technique to assess the impact of dendritic branching on the mode of self-assembly. Compound **G1-C12-G1** gave rise to a sample spanning network of “sausage-like” morphologies (Figure 5a). These sausages were relatively thick (ca. 120 nm) but did show some evidence of unidirectional growth. Gelator **G3-C12-G3**, on the other hand, formed nanoscale morphologies with tangled fibers more typical of a gel (Figure 5c). Unfortunately, despite repeated attempts, **G2-C12-G2** could not be imaged by SEM. We have previously had similar problems with certain gelators.[15] It was possible, however, to image **G2-C6-G2** with the shorter spacer chain, and this image is shown in Figure 5b. Once again a fibrillar morphology was observed for this system. These observations confirm that the differences in thermal stability between **G1** and **G2/3** systems can be attributed to the higher generation dendrimers forming more effective interpenetrated sample-spanning networks. The **G2** and **G3** systems appear to have higher predispositions for anisotropic self-assembly driven by the multiple hydrogen bonding groups inherent within their dendritic architectures.

To probe the morphologies observed by SEM, small-angle X-ray scattering (SAXS) was performed. The SAXS intensity $I(q)$ of a solution corresponding to a system of interacting cylindrical particles can be written as eq 1, where N is the average number density of scattering particles, $P(q)$ is the form factor of the particle and $S(q)$ is the structure factor of the system, which tends to unity for diluted noninteractive systems.

$$I(q) = NP(q)S(q) \tag{1}$$

In the case of a solution of homogeneous infinite solid cylinders of radius R_c and length L, with polydisperse cross section, the form factor is given by eq 2,[23] where $J_1(qr)$ is the Bessel function of first order and $(\sigma/R_c)\cdot 100$ is the polydispersity in R_c.

$$P(q) = \int_0^{\infty} \frac{J_1(qr)^2}{r^2 q^3} \exp\left[\frac{-(r - R_c)^2}{2\sigma^2}\right] dr \tag{2}$$

Unfortunately, there is no analytical expression in the literature for the structure factor of a system of interacting cylindrical particles. Therefore we modeled $S(q)$ as a Gaussian function, centered at q_0 and with full width at half-height w, in an attempt to empirically approximate the interaction effects between the particles (eq 3).

$$S(q) = \exp\left\{-2\left[\frac{q - q_0}{w}\right]^2\right\} \tag{3}$$

Finally, a background contribution, given by eq 4 (where A, B, and C are adjustable parameters), was considered to dominate the SAXS curve at large q. In the following, we focus on the cylinder radius R_c and its corresponding polydispersity. However, all parameters used to model the SAXS data are given in the Supporting Information.

$$I_b(q) = Aq^B + C \tag{4}$$

Figure 6a and b shows the results obtained for the modeling of the SAXS curves for **G1-C12-G1** at 25 and 47 °C, respectively. Structure factor effects in the SAXS curve were found to be negligible and the data was modeled using eqs 1 and 2, with $S(q) = 1$. Although the scattering profiles are different at the two temperatures, the radius of the self-assembly, modeled as infinite solid cylinders (R_c) remains the same at 72 Å, while the polydispersity grows from 3.2% to 3.6%. Since

---

(21) For an overview of CD spectroscopy, see: Berova, N.; Nakanishi, K.; Woody, R. W. *Circular Dichroism: Principles and Applications*, 2nd ed.; Wiley-VCH: Weinheim, 1994.

(22) For selected examples, see: (a) Snip, E.; Shinkai, S.; Reinhoudt, D. N. *Tetrahedron Lett.* **2001**, *42*, 2153-2156. (b) Ihara, H.; Takafuji, M.; Sakurai, T.; Katsumoto, M.; Ushijima, N.; Shirosaki, T.; Hachisako, H. *Org. Biomol. Chem.* **2003**, *1*, 3004−3006. (c) Hanabusa, K.; Maesaka, Y.; Kimura, M.; Shirai, H. *Tetrahedron Lett.* **1999**, *40*, 2385−2388.

(23) *Small-Angle X-ray Scattering*; Glatter, O.; Kratky, O., Eds.; Academic Press: London, 1982.

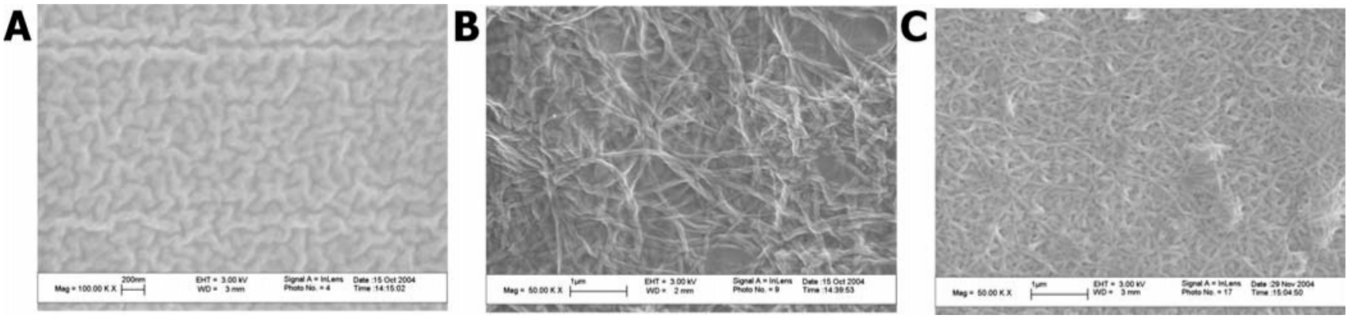

Figure 5. Scanning electron microscopy (SEM) images of (a) **G1-C12-G1** (scale bar = 200 nm), (b) **G2-C6-G2** (scale bar = 1 μm), and (c) **G3-C12-G3** (scale bar = 1 μm).

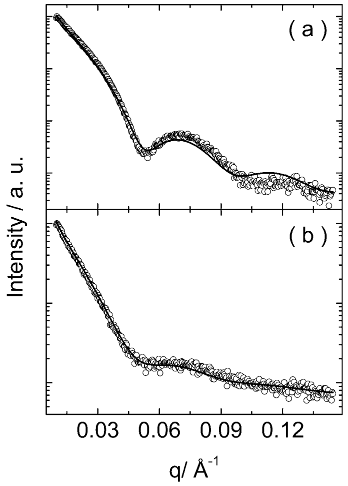

Figure 6. (○) SAXS data for **G1-C12-G1** at (a) 25 and (b) 47 °C. The full lines correspond to the modeling using equations 1 and 2, with $S(q) = 1$, and considering a background $Aq^B + C$. Conc = 20 mM, solvent = toluene.

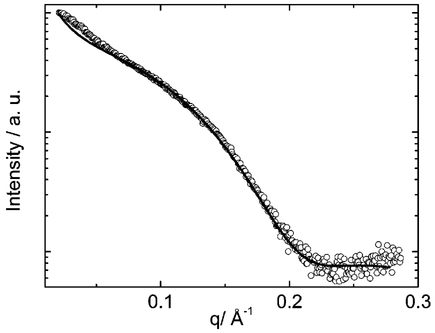

Figure 7. (○) SAXS data for **G2-C12-G2** at 22 °C. The full lines correspond to the modeling using eqs 1−3 and considering a background $Aq^B + C$. Conc = 20 mM, solvent = toluene.

Table 2. Parameters Used to Model the SAXS Data

fig	sample	T (°C)	R_c (Å)	σ/R_c (%)	A	B	C	w (Å^{-1})	q_0 (Å^{-1})
6a	$\mathbf{G_1C_{12}G_1}$	25	72	3.2	0.0015	−1.86	0		
6b	$\mathbf{G_1C_{12}G_1}$	47	72	3.6	0.079	−1.13	0.43		
7	$\mathbf{G_2C_{12}G_2}$	22	17.5	9	0.07	−0.4	0	0.1717	0.163

the SAXS intensity is given in arbitrary units, the only relevant parameter to the background is B, which changed from −1.86 to −1.13 when the temperature was increased from 25 to 47 °C. It is interesting to note that the relatively large value of R_c obtained for **G1-C12-G1** is in broad agreement with the morphology observed by SEM, which indicated the formation of a sausage-like morphology with relatively large nanoscale features.

Figure 7 shows the results obtained for the modeling of the SAXS curve for **G2-C12-G2** at 22 °C. Structure factor effects dominated the SAXS curve at low scattering vectors, and therefore the data was modeled using eqs 1−3. Our results indicate that $R_c = 17.5$ Å with a polydispersity of 9% ($q_o = 0.1615$ Å^{-1}, $w = 0.1517$ Å^{-1}, and $B = 0.4$). This smaller value of R_c is in approximate agreement with the expected dimensions of an individual second generation dendritic building block modeled using Spartan Pro simulations. This suggests that, for **G2-C12-G2**, the self-assembled state underpinning gelation is constructed from cylinder-like anisotropic objects that have the width of a single dendrimer building block.

The SAXS data presented in this work has not been transformed to absolute intensity scale. Therefore, $N = 1$ was arbitrarily fixed in eq 1. The parameters used to model the SAXS data in the figures indicated are listed in Table 2.

Comparison of One- and Two-Component Systems: Dendritic Effects. A unique feature of these gelators is that they can be *directly* compared with the two-component analogue reported previously,[7−12] the first system amenable to such a treatment.

Comparison 1. G1-C*n*-G1 forms gels, but **G1···C*n*···G1** does not. The one-component system has a *higher propensity to hierarchically self-assemble* than its two-component analogue. The lack of macroscopic gelation for **G1···C12···G1** suggests that the thermodynamics of the process are not sufficiently favorable to induce a sample-spanning network. There are two possible reasons for this:

- The one-component system has two *extra amide groups*. As shown in Figure 4, these groups are involved in crucial intermolecular hydrogen bond interactions for the first generation system, which will enthalpically favor the self-assembly of the one-component gelator.
- The one-component system, unlike its two-component analogue, does not have to initially assemble into a complex before hierarchical self-assembly. This should also give the one-component system a greater propensity for gelation as there is a smaller entropic penalty for its self-assembly.

We argue that both of these factors probably play an important role in controlling differences between the one- and two-component gelators. It is interesting to note that SEM images of dried **G1···C12···G1** did illustrate a sausage-like morphology,[9] directly analogous to that reported here for **G1-C12-G1** (Figure 5a), suggesting that even though macroscopic gelation

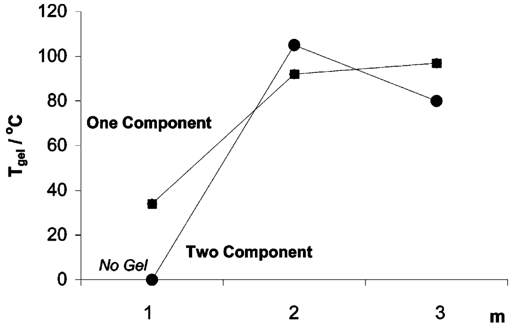

Figure 8. Graph showing the relationship between dendritic generation and T_{gel} (plateau region) for both one- and two-component **C12** gelation systems. Solvent = toluene.

is not observed, the two-component system does have some potential to aggregate in a manner similar to its one-component analogue.

Comparison 2. G2-C12-G2 is able to gelate $CHCl_3$, but **G2···C12···G2** cannot.[10] This observation is in agreement with the discussions above that explain why the one-component system has a greater propensity for forming gels.

Comparison 3. The branching in **G*m*-C12-G*m*** has a positive dendritic effect up to the third generation, but in **G*m*···C12···G*m*** the second generation system is optimum (Figure 8).[9]

Different dendritic gelators reported in the literature exhibit different types of dendritic effect: negative,[5g] optimum,[5e,f,k,9] and positive.[15] We have previously argued[9] that dendritic gelation effects can be rationalized in terms of a balance between

- additional enthalpically *favorable* interactions (e.g., hydrogen bonds) at higher generation,
- enthalpically *unfavorable* steric interactions at higher generation, and
- entropically *unfavorable* terms associated with the immobilization of larger dendritic systems.

The balance of these factors will be fundamentally different for one- and two-component systems, and furthermore, an additional factor applies specifically to the two-component system:

- the *interaction* between the two components may vary on increasing the dendritic generation.

It is therefore perhaps not surprising that one- and two-component gelators have different dendritic effects up to the third generation.

Characterization of the Novel Gel-Phase Materials. (b) Effect of Spacer Chain Length. For **G1-C*n*-G1**, increasing the length of the spacer chain increased the T_{gel} value in the plateau region (Figure 9). In a number of previous reports, an odd−even effect of aliphatic spacer chain length on gel properties has been reported,[24] but in this case the thermal stability of the gel increased incrementally on increasing the length of the spacer chain. However, this effect was relatively small; increasing the spacer chain from **C6** to **C12** only increased T_{gel} by 8 °C, from 26 to 34 °C.

The second generation gelators **G2-C6-G2**, **G2-C9-G2**, and **G2-C12-G2** were also investigated (Figure 10). Increasing the length of spacer chain from **C6** to **C12** increased the T_{gel} value in the plateau region from 60 °C (**C6**) to 92 °C (**C12**). Increasing the length of the spacer chain also decreased the concentration of dendrimer required for effective gelation (i.e., the plateau region occurs at concentrations of 25 mM for **G2-C6-G2**, 20 mM for **G2-C9-G2**, and 15 mM for **G2-C12-G2**).

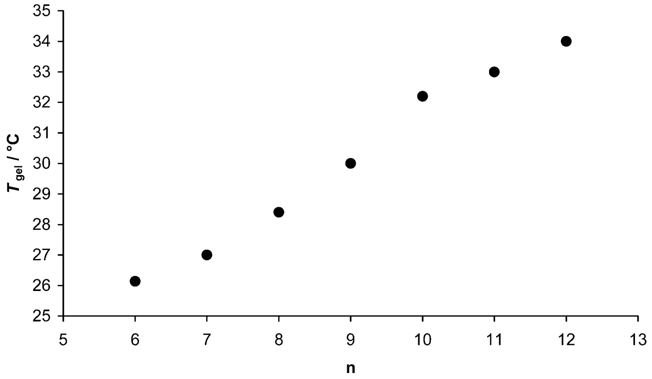

Figure 9. Effect of spacer chain length on T_{gel} for gels based on **G1-C*n*-G1**. Conc = 60 mM, solvent = toluene.

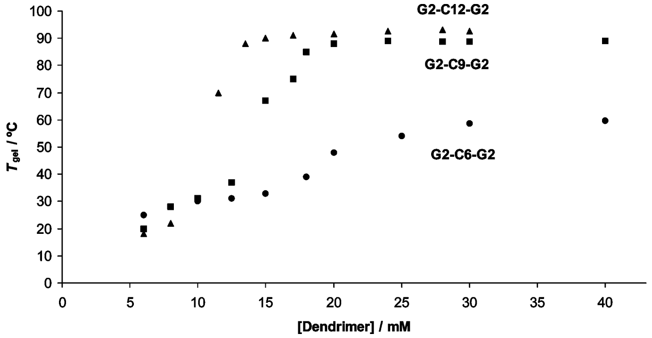

Figure 10. Effect of [dendrimer] on the gel−sol transition temperature (T_{gel}) for **G2-C*n*-G2** as measured by tube-inversion methodology. Solvent = toluene.

There are two possible reasons for these effects of spacer chain:

- there are additional van der Waals forces present when using longer spacer chains, and
- longer spacer chains confer an optimal spatial arrangement of dendritic headgroups that promotes the formation of intermolecular hydrogen bonding.

^{1}H NMR experiments also offered a powerful insight into the role of spacer chain in the assembly process. The N−H resonances of the **G1-C*n*-G1** series of gelators (all at concentrations of 60 mM) were compared. For gelators with longer spacer chains, the N−H peaks appeared further downfield (Figure 11). The N−H protons are therefore more strongly involved in forming intermolecular hydrogen bond interactions as the spacer chain length increases. Interestingly, the carbamate protons were slightly more strongly affected ($\Delta\delta = 0.34$ ppm) than the amide groups ($\Delta\delta = 0.32$ ppm). This indicates that the spacer chain exerts its effect on macroscopic thermal stability by allowing the optimization of the hydrogen bond interactions, particularly those secondary interactions involving the carbamate groups in the dendritic head units (in particular the carbamate group at ca. 5 ppm).

CD spectroscopy provided further support for the ability of the spacer chain to enable effective interactions between the chiral dendritic headgroups. All **G1-C*n*-G1** gelators exhibited negative CD peaks with λ_{max} values of ca. 220 nm, ascribable

---

(24) (a) Tomioka, K.; Sumiyoshi, T.; Narui, S.; Nagaoka, Y.; Iida, A.; Miwa, Y.; Taga, T.; Nakano, M.; Handa, T. *J. Am. Chem. Soc.* **2001**, *123*, 11817−11818. (b) Sumiyoshi, T.; Nishimura, K.; Nakano, M.; Handa, T.; Miwa, Y.; Tomioka, K. *J. Am. Chem. Soc.* **2003**, *125*, 12137−12142.

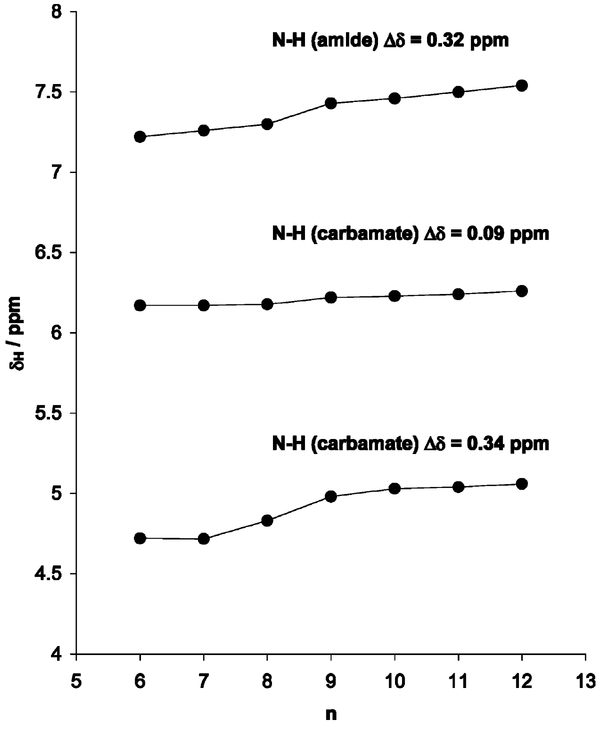

Figure 11. NMR shift of N−H protons for **G1-C*n*-G1**, illustrating the effect of spacer chain on the extent of dendrimer−dendrimer hydrogen bonding. All spectra were measured at a temperature of 20 °C and with [dendrimer] = 60 mM. Solvent = toluene-d_8.

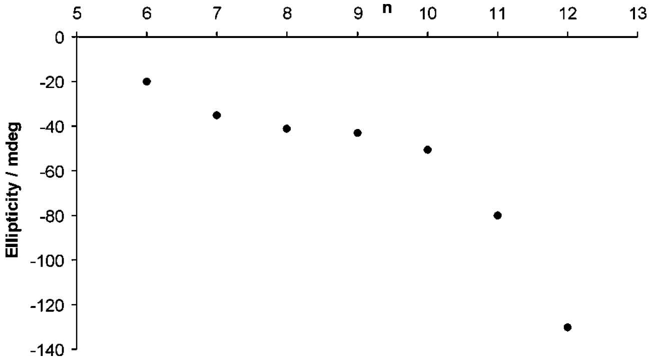

Figure 12. Intensity of the CD band observed at 220 nm for **G1-C*n*-G1** illustrating the effect of spacer chain on ellipticity. All spectra were recorded with [dendrimer] = 3 mM. Solvent = cyclohexane.

to the organization of amide bonds within a chiral environment. The dramatic increase in ellipticity on increasing the spacer chain from **C6** to **C12** indicates that the spacer chain has a profound effect on the level of chiral organization present in the self-assembled state (Figure 12).

For **G2-C*n*-G2** a similar trend was observed (Figure 13), with the increase in chiral organization being, if anything, even more dramatic. The **G2-C6-G2** aggregated state was effectively achiral, even though the individual gelator building blocks are composed of chiral centers. This is a surprising result, particularly given that **G2-C6-G2** is a potent gelator (T_{gel} = 60 °C) and obviously forms a fibrous assembly (Figure 5b). Increasing the length of the spacer chain from **C9** to **C12** dramatically enhanced the chiral ordering (i.e., helicity) on the nanoscale, even though the thermal properties of these two gels in the plateau region are very similar.

For both **G1** and **G2** systems, the nanoscale chirality is highly dependent on the spacer chain length, but the observed macroscopic T_{gel} values only vary slightly! We argue that the "new" covalent amide groups provide the primary molecular recognition pathway for the assembly of these one-component gelators into fibers, and hence control the aspect ratio and thus thermal stability; therefore, T_{gel} values vary little between the different gelators. However, we propose that there is a secondary molecular recognition pathway involving hydrogen bond interactions between the chiral dendritic headgroups (Figure 14). We propose that these interactions play a secondary role in the formation of a sample spanning network, yet they are of great importance in controlling the organization present within the fiber (e.g., chiral ordering). Changing the spacer chain optimizes these secondary interactions and therefore, although having only a small effect on the macroscopic thermal behavior of the gel, has a major effect on carbamate hydrogen bonding and thus on nanoscale chiral organization. For example, whereas **G2-C6-G2** clearly forms an effective fibrous assembly (Figure 5b), the chiral molecular scale information is not transcribed into the fibers because the short spacer chain makes the dendrimer relatively inflexible and hence unable to organize the chiral information into a well-structured form (e.g., a helix). Only with a longer spacer chain (e.g., **C12**) do the dendritic headgroups have sufficient flexibility to achieve effective chiral organization.

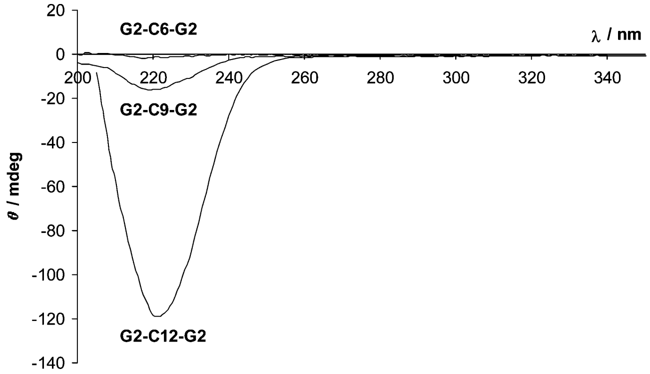

Figure 13. CD spectra of **G2-C*n*-G2** illustrating the effect of spacer chain on the magnitude of the circular dichroism band. [Dendrimer] = 3 mM. Solvent = cyclohexane.

It is therefore likely that the role of the spacer chain in mediating gelation is that a longer spacer chain enables the dendritic headgroups to achieve a much greater degree of chiral order via more spatially effective hydrogen bond interactions. This is presumably a consequence of the increasing length of the spacer chain decreasing the steric hindrance between dendritic headgroups.

Comparison of One- and Two-Component Systems. Effect of Spacer Chain. Comparison 1. One- and two-component gels have different degrees of tunability (Figure 15). For the one-component second generation system, increasing the spacer chain from **C6** to **C12** only increases the T_{gel} value from 60 to 92 °C but causes a dramatic change from 4 to 105 °C for the two-component analogue.[8] In terms of thermal strength, the two-component system is more tunable than its one-component analogue, and interestingly, the one-component system is therefore not always a more effective gelator than its two-component analogue. For example, **G2-C12-G2** (T_{gel}, 92 °C) is actually a less effective gelator than **G2···C12···G2** (T_{gel}, 105 °C).

In the one-component system, the "locked-in" "new" amide groups provide an additional molecular recognition pathway,

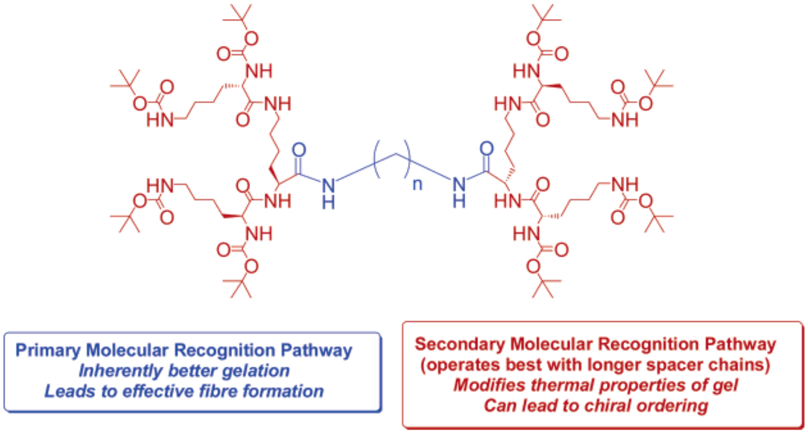

Figure 14. Summary of the types of molecular recognition occurring in the novel one-component gelators. For the two-component analogues, the primary molecular recognition pathway is absent (as the amide bonds are replaced by acid−amine interactions that hold the complex together).

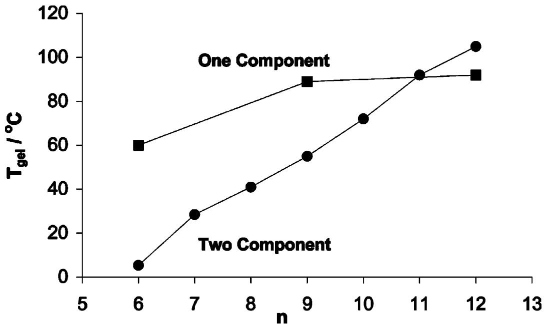

Figure 15. Graph showing the relationship between spacer chain and T_{gel} (plateau region) for both one- and two-component **G2** gelation systems. Solvent = toluene.

with the effective organization of dendritic headgroups playing a secondary role. The two-component system, however, does not have these amide groups; indeed in this case, the anisotropic self-assembly is solely dependent on the optimal organization of the dendritic headgroups. This means that the effect of spacer chain, which allows the optimization of dendrimer-dendrimer hydrogen bond interactions, is much more important for the two-component system than its one-component analogue. We propose that the greater ability to reorganize and maximize the strength of hydrogen bonding interactions means that certain two-component gelation systems (such as **G2···C12···G2**) are actually better gelators than their one-component analogues, even though the key covalent amide groups are absent.

Comparison 2. For the one-component system, the fibers are not always chirally organized on the nano level, whereas they are for the two-component system.[8] For the one-component system (especially **G1**), the covalent amides dominate the self-assembly process and always allow fiber formation irrespective of whether the dendritic headgroups are able to achieve effective nanoscale chiral organization. Indeed, with a short spacer chain, the chiral dendritic headgroups are unable to organize themselves into a helical array within the fibers. Only with longer spacer chains does chiral organization become possible as a consequence of a decrease in steric crowding.

For the two-component analogue, whenever gelation is observed it is always accompanied by nanoscale chiral ordering. Indeed, effective fiber formation and chiral ordering are only observed with longer spacer chains. With shorter spacer chains, such as **G2···C6···G2**, neither fiber formation nor chiral ordering are observed,[8] whereas for **G2-C6-G2** the assembly process gives rise to fibers which are effectively achiral. In the two-component system, the covalent amides are absent, and fiber formation is completely dependent on intermolecular hydrogen bonding between the chiral dendritic headgroups, which therefore *must* be effectively organized for the formation of high aspect ratio fibers to be favored.

Conclusions

A novel family of one-component dendritic gelators has been reported, and the ability of these molecules to self-assemble into nanostructured gel-phase materials was investigated using thermal measurements, ^{1}H NMR and CD spectroscopy, SEM, and SAXS. Dendrimers of all generations formed effective gels under ambient conditions. The gelators exhibited a positive dendritic effect on the thermal properties of gelation up to the third generation. It was also shown that longer spacer chains enabled the formation of slightly stronger gels with a greater degree of dendrimer−dendrimer hydrogen bonding, as well as dramatically enhanced supramolecular chiral organization.

Importantly, these systems were compared against their direct two-component analogues, the data for which have been reported in a recent series of papers.[7−12] It was found that the one-component systems are generally inherently better gelators. Potential reasons for the greater ability of the one-component system were discussed: the additional covalent amide groups can form favorable intermolecular hydrogen bond interactions, and there is also less entropic cost to the self-assembly process.

The fact that the “new” amide groups act as a key molecular recognition pathway for the assembly of the one-component gelator into fibers has a direct effect on the transcription of chirality from the molecular scale to the nanoscale. For example, **G2-C6-G2** formed an effective fibrous assembly, but the fibers themselves were achiral on the nanoscale. Only with longer spacer chains (e.g., **G2-C12-G2**) was the transcription of chirality into the fibers switched on, as the system became more flexible and hence better able to organize the chiral dendritic headgroups (which act as the secondary molecular recognition pathway for fiber formation).

In the absence of “locked-in” covalent amides at each end of the spacer chain, the two-component system relies solely on dendrimer−dendrimer intermolecular hydrogen bond interactions for its self-assembly into fibers. As a consequence, this system is significantly more tunable and sometimes even forms thermally more stable materials than its one-component analogue. For the two-component system, fiber formation is wholly dependent on intermolecular hydrogen bond interactions between the dendritic headgroups and is therefore always accompanied by chiral organization.

In summary, this paper, by comparing structurally analogous one- and two-component self-assembling dendrimers, has illuminated the molecular recognition pathways that control fibril formation and provided real insight into the similarities and differences between one- and two-component gelation systems.

Acknowledgment. We thank the Leverhulme Trust for supporting this research through the provision of a postdoctoral fellowship (A.R.H.). We also thank John Harrington (Leeds Electron Microscopy and Spectroscopy Centre (LEMAS), Department of Materials, University of Leeds) for assistance with scanning electron microscopy.

Supporting Information Available: Full experimental information, including materials, methods and characterization data for all new gelators; differential scanning calorimetry traces; and circular dichroism spectra. This material is available free of charge via the Internet at http://pubs.acs.org.

JA050412D